New empirical backscattering models for estimating bare soil surface parameters

S. Mohammad Mirmazloumi , Mahmod Reza Sahebi & Meisam Amani

Published online: 20 Dec 2020.

Submit your article to this journal

View related articles

View Crossmark data

Taylor & Francis
Taylor & Francis Group

Check for updates

New empirical backscattering models for estimating bare soil surface parameters

S. Mohammad Mirmazloumi [a], Mahmod Reza Sahebi [b] and Meisam Amani [c]

aGeomatics Division, Centre Tecnològic De Telecomunicacions De Catalunya (CTTC/CERCA), Castelldefels, Spain; bFaculty of Geodesy and Geomatics Engineering & Remote Sensing Institute, K. N. Toosi University of Technology, Tehran, Iran; cWood Environment & Infrastructure Solutions, Ottawa, ON, Canada

ABSTRACT

Various models have been proposed to estimate the degree of backscatter in Synthetic Aperture Radar (SAR) images. However, it is still necessary to calibrate these models based on the characteristics of different study areas and to propose new models to achieve the highest possible accuracy in estimating the backscattering coefficient (σ^0) SAR. In this study, three empirical models, including Champion, Sahebi and Zribi/Dechambre, were initially calibrated for two SAR datasets (i.e. The Airborne Synthetic Aperture Radar (AIRSAR) and Canadian Space Agency radar satellite (RADARSAT-1)) acquired over two bare soil study areas with various soil characteristics. The Zribi/Dechambre model was then modified by revising the roughness parameter to obtain higher accuracy in estimating σ^0 over a larger range of incidence angles (θ). A new empirical model was also proposed by combining the four parameters of Soil Moisture (SM), standard deviation of surface height -root mean square- (rms), correlation length (l), and θ. To this end, the most appropriate form of the regression model was investigated and used for each of these parameters to obtain the highest correlation between the *in-situ* data and σ^0 values. A comparison of the empirical models showed that the modified Zribi/Dechambre had the highest accuracy in predicting σ^0 values with the Root Mean Square Errors (RMSE) of 1.20 dB and 1.59 dB over Oklahoma and Quebec, respectively. Furthermore, coefficients values of the new proposed model remained stable in the two datasets unlike the other investigated models. In this study, the effects of l on the accuracy of the new proposed model were also assessed. It was concluded that l had a considerable impact on the accuracy of the proposed model and including this parameter can improve the accuracy by up to 1 dB.

1. Introduction

Synthetic Aperture Radar (SAR) is an active microwave imaging system that sends microwave pulses to acquire information from the surface of the Earth. This system uses the forward motion of a spacecraft to synthesize a much longer antenna and, thus, to provide high spatial resolution datasets (Hosseini and Saradjian 2011). The acquisition of high-

CONTACT S. Mohammad Mirmazloumi ✉ sm.mirmazloumi@cttc.es Geomatics Division, Centre Tecnològic De Telecomunicacions De Catalunya (CTTC/CERCA), Castelldefels 08860, Spain

resolution, multi-dimensional, and multi-mode datasets by new SAR systems has posed many challenges in the processing and interpretation of the corresponding datasets (Sun, Shimada, and Xu. 2017). However, SAR images contain valuable information about their targets, making them unique compared to other remote sensing datasets. For example, SAR data are great resources for estimating soil parameter because SAR signals are highly sensitive to the soil dielectric constant and surface roughness (Ulaby, Dubois, and Van Zyl 1996; Sahebi, Bonn, and Bénié 2004; Azimi et al. 2020). SAR can also collect data in almost any atmospheric condition, which makes it a suitable option in areas with frequent cloud cover and bad weather conditions (Amani et al. 2018; Zakharov et al. 2020). Moreover, SAR microwave signals can penetrate not only clouds, but also vegetation canopies and soil surfaces and, therefore, acquire information from areas invisible in other satellite imagery, such as optical satellite data (Mahdavi et al. 2017). Open-access SAR data, such as Sentinel-1 imagery, has facilitated frequent and high-resolution soil moisture retrieval (El Hajj et al. 2019; Hachani et al. 2019; Ezzahar et al. 2020; Zhang et al. 2020). Consequently, SAR has been utilized in different environmental applications, including Earth surface monitoring, land cover classification, geohazard events monitoring, climate change analysis, and drought monitoring (Berardino et al. 2002; Tofani et al. 2013; Amani et al. 2017; Li et al. 2020).

SAR systems generally collect the backscattering coefficient (σ^0) from different targets. The fraction σ^0 describes the amount of average backscattered energy compared to the energy of the incident field. This parameter depends on the SAR configuration (e.g. incidence angle (θ) and wavelength (λ)) and the target properties (e.g., Soil Moisture (SM) content and soil surface roughness) (Champion 1996). Linear correlation of radar signal and SM was first investigated as a function of co-polarized C-band configuration by Ulaby and Batlivala (1976). Later, considering the depth of soil, stronger sensitivity of radar signal to SM was observed using a linear relationship (Attema and Ulaby 1978) and empirical or physical radar backscattering models (Oh, Sarabandi, and Ulaby 2004; Fung, Li, and Chen 1992; Dubois, Van Zyl, and Engman 1995; Baghdadi, Aubert, and Zribi 2011), which present an increase of radar signal with SM. Different models have been developed to formulate the relationship between σ^0 and land surface parameters, which are generally called backscattering models. Over the past 40 years, many backscattering models, from simple linear to complex theoretical models, have been proposed based on radar data availability and different *in-situ* datasets (e.g., Attema and Ulaby 1978; McNairn et al. 1996; Baghdadi et al. 2012; MirMazloumi and Sahebi 2016; Mirsoleimani et al. 2019; Ezzahar et al. 2020). In case of the effects soil roughness and θ on the radar signal, although low θ minimizes the effect of soil roughness (Verhoest et al. 2008), roughness estimation is more accurate for $\theta > 30°$ (Bousbih et al. 2017). Furthermore, low to medium values of θ (i.e., 20°to35°) have been suggested an optimal range to estimate SM (Holah et al. 2005). Since relationship between σ^0 and surface roughness and moisture are not linear (Zribi et al. 2013), several studies have proposed logarithmic (Sahebi, Bonn, and Bénié 2004) and exponential terms (Zribi and Dechambre 2003; Baghdadi, Holah, and Zribi 2006; Baghdadi et al. 2007) to highlight the impacts of surface roughness on σ^0 (Petropoulos, Ireland, and Barrett 2015).

Backscattering models are generally divided into three categories: empirical, semi-empirical, and theoretical or physical (MirMazloumi and Sahebi 2016). Theoretical back-scattering models, such as the Integral Equation Model (IEM) (Fung, Li, and Chen 1992),

Small Perturbation Model (SPM) (Ulaby, Moore, and Fung 1982; Hajnsek, Pottier, and Cloude 2003; Iodice, Natale, and Riccio 2011), Geometrical Optic Model (GOM) (Ulaby, Moore, and Fung 1982), and Physical Optic Model (POM) (Ulaby, Moore, and Fung 1986) are relatively complex and there are several limitations to obtain high accuracy in estimating soil parameters from these models. However, physical models have been applied to provide site-independent relationships (Baghdadi et al. 2004), indicating their sensitivity to dielectric constant and roughness (Baghdadi et al. 2012), as well as their independency to specific site calibration (Mirsoleimani et al. 2019). For instance, it is challenging to apply the IEM model to estimate SM content over a large area because surface roughness is not usually well described by the statistical representations used in this model (Zribi et al. 2000; Davidson et al. 2003; Callens, Verhoest, and Davidson 2006). Moreover, additional information, such as topography and soil type are required to optimize the performance of IEM (Zribi and Dechambre 2003; Notarnicola and Solorza 2014). Furthermore, the validity domain of SPM, GOM, and POM are restricted to a limited surface roughness range. These models have been generally employed for smooth or rough surfaces. Although Hajnsek, Pottier, and Cloude (2003) and Iodice, Natale, and Riccio (2011) have proposed second-order polarimetric scattering models to expand the validity range of SPM, they were only designed for cross-polarization and were not suitable for short wavelength C-band (Hajnsek, Papathanassiou, and Cloude 2001; Barrett, Dwyer, and Whelan 2009). Therefore, the estimation of soil surface parameters using theoretical models requires very detailed knowledge of surface roughness, which is only achievable through intensive roughness measurement campaigns. Semi-empirical models, such as Oh (2004) and Dubois (Dubois, Van Zyl, and Engman 1995), on the other hand, require a large amount of field data to accurately model the nonlinear response of SAR backscattering to SM and surface roughness parameters (Zribi, Gorrab, and Baghdadi 2014; Petropoulos, Ireland, and Barrett 2015). Moreover, there are limitations to invert the physical part of the semi-empirical models to a specific geographic area with similar roughness characteristics (Baghdadi, Holah, and Zribi 2006; Paloscia et al. 2008).

Compared to theoretical and semi-empirical models, empirical models are often favoured by users because they are straightforward to implement and can easily invert σ^0 to soil surface parameters (Zribi and Dechambre 2003; Gherboudj et al. 2011; Rao et al. 2013; Chai et al. 2015; Kirimi et al. 2016). The simplest empirical model was developed to represent the relationship between SM and radar response (Attema and Ulaby 1978). In fact, many of the first empirical models were generally proposed based on the linear relationship between σ^0 and SM when SM content values were between about 10% and 35% and under the assumption that roughness does not change between successive radar measurements (Wang and Qu 2009; Zribi et al. 2013). An exponential term was then included in the linear relationship to consider the effects of roughness on σ^0 and, thus, to make empirical models more applicable (Zribi and Dechambre 2003; Baghdadi, Holah, and Zribi 2006; Baghdadi, Aubert, and Zribi 2011; Zribi et al. 2013). During that time, several other ideas were also proposed to improve the efficiency of empirical models. For examples, Baghdadi, Aubert, and Zribi (2011) and Baup et al. (2011) suggested that considering the difference between one image acquired during the wet season and

a reference image acquired during the dry season could further eliminate the effects of surface roughness.

Although many empirical backscattering models have been developed, their applicability and accuracy should be investigated in different study areas. This is because the coefficients of empirical models are usually calculated using specific *in-situ* datasets over a study area. Accordingly, these models may need to be refined or new empirical models developed to obtain reasonable accuracies in other regions. Thus, in this study, three empirical backscattering models, including those proposed by Champion (1996), Sahebi, Bonn, and Gwyn (2003), and Zribi and Dechambre (2003) were first investigated in study areas in Oklahoma, USA and in Quebec, Canada. Then, the coefficients of these models were calibrated to obtain better accuracies based on characteristics specific to the study areas. Furthermore, a modified version of the Zribi/Dechambre model (Zribi and Dechambre 2003) and a new empirical backscattering model that is a function of SM, θ, standard deviation of surface height – root mean square – (rms), and correlation length (*l*) were proposed to obtain the most accurate estimation of σ^0 over the study areas.

2. Study areas and data

2.1. Study areas

The datasets from three bare soil regions were used in this study to consider soil types with various characteristics in the backscattering models. The first study area (Figure 1 (*a*)) was the Little Washita Experimental Watershed (LWREW) with an area of 611 km^2, located in Oklahoma in the Southern Great Plains of the United States (34° 57′ N, 98° 01′ W). In this study area, summers are typically long, hot, and relatively dry and winters are generally short, temperate, and dry but are usually very cold for a few weeks. The topography of the LWREW is moderately rolling with a maximum relief less than 200 m. Except for a few rocky and steep hills near the Cement region, the upland topography is gently to moderately rolling. Furthermore, soils include a wide range of textures. Land use in this watershed is also dominated by rangeland and pasture (63%) with large areas of winter wheat and other croplands concentrated in the floodplain and western portions of the watershed (Jackson et al. 2002).

The second study area includes the Chateauguay River (45° 19′ N, 73°46′ W) and Pike River (45° 08′ N, 72° 54′ W) watersheds (i.e., the CRPRW study area). This study area is located on the south shore of the St. Lawrence River, southeast of Montréal, Quebec, Canada (Figure 1(b)). This region contains many agricultural fields on a relatively flat and relief plateau with a homogeneous soil texture composed of about 36% clay, 42% silt and 22% sand (Sahebi, Bonn, and Gwyn 2003).

2.2. In-situ datasets

In-situ datasets collected over the study areas were used to evaluate the accuracy of the empirical models (see Table 1 for the amount of field data). The field data from LWREW were collected by the Soil Moisture Experiments (SMEX03) administration and campaign members. SMEX03 stations are equipped with different types of sensors to measure
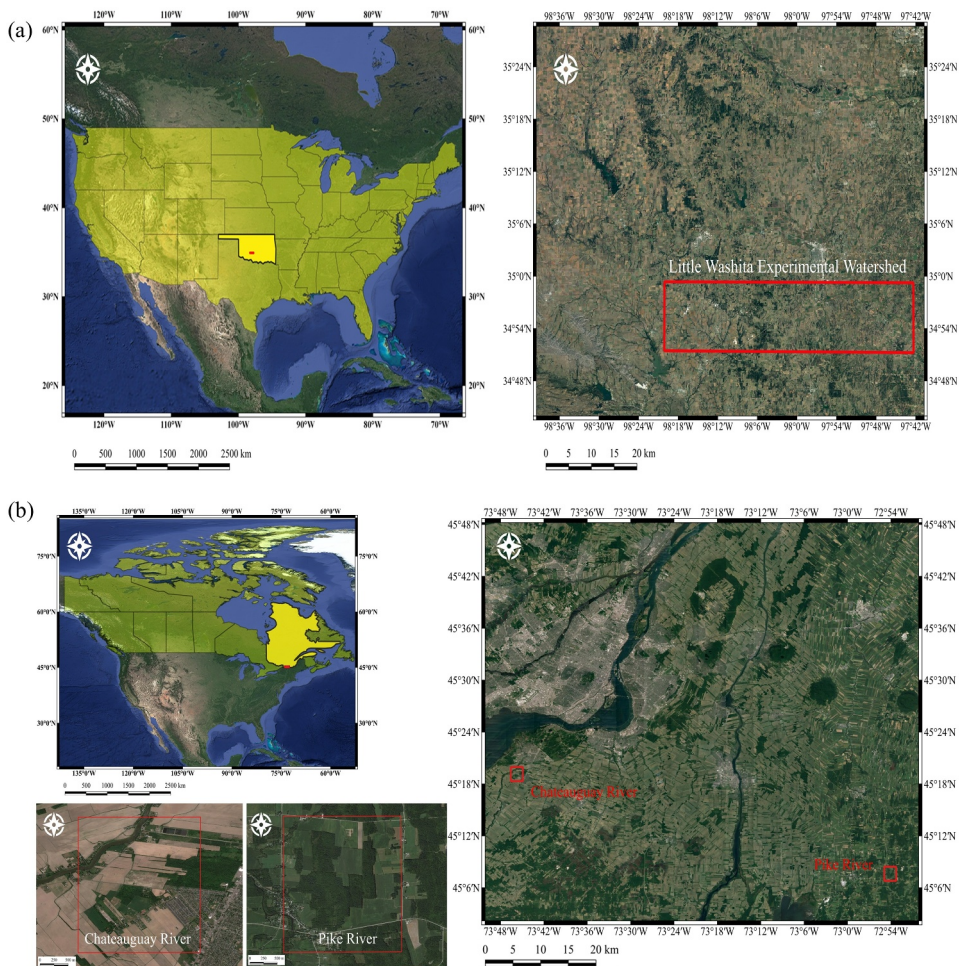
Figure 1. Study areas: (a) Little Washita Experimental Watershed (LWREW) and (b) Chateauguay River and Pike River watersheds (CRPRW).

Table 1. Number of *in-situ* datasets and ranges of parameters.

Dataset	Number of samples	Number of trains	Number of tests	rms (cm)	GSM (g g-1) *	Correlation length (cm)
LWREW	52	39	13	0.60 to 3.70	0.03 to 0.30	1.90 to 9.00
CRPRW	39	29	10	0.80 to 4.80	0.14 to 0.34	1.50 to 39.00

*Gravimetric soil moisture in grams of water per grams of dry soil (gg^{-1})

parameters such as the dielectric constant, volumetric and gravimetric SM contents, soil temperature, bulk density, and soil surface roughness (Jackson et al. 2002). In this study, only the volumetric SM at the depth of 0 to 6 cm and soil surface roughness collected over 13 sites were considered. A ThetaProbe™ sensor was used to measure SM content. The rms height (0.2 to 2.6 cm) and *l* (1.9 to 7.5 cm) were also calculated through analysing the digitized photographs using the method described in Jackson and Cosh (2006).

Table 2. Description of the remote sensing datasets.

Study area	Satellite	Acquisition date	Band / polarization	Incidence angles (°)	Spatial resolution (m, range × azimuth)
LWREW	AIRSAR	03 July 2003	C / HH	[47 to 64]	6.60 × 9.26
CRPRW	RADARSAT-1	12 December 1999	C / HH	[20 to 25]	20 × 27
		18 December 1999		[40 to 49]	

The *in-situ* data collected over CRPRW study area, also included SM and surface roughness data over 27 sites. A ThetaProbe™ soil moisture sensor, which measured the apparent dielectric constant, was used to derive the SM content at a depth of 0 to 5 cm (dictated by the length of the probe's needle). Using the equation presented in the ThetaProbe SM user manual, the direct outputs (DC voltage in mV) were converted to soil water content ($m^3 \ m^{-3}$) and dielectric constant. Moreover, six 2 m long surface profiles with 1 cm sampling intervals (three parallel and three perpendicular to the soil furrows) were used at each site to calculate the height of the rms (1.5 to 5.4 cm). The method to extract and model roughness parameters is described in detail in Beaulieu, Leclerc, and Moisan (1995).

2.3. Remote sensing datasets

The information about the satellite images used in this study is provided in Table 2. Two types of SAR datasets were used in assessing the backscattering models to obtain a more comprehensive conclusion about the accuracy and limitations of each backscattering model. These images were acquired at the same time as the *in-situ* data measurements. Four the Airborne Synthetic Aperture Radar (AIRSAR) and two Canadian Space Agency radar satellite (RADARSAT-1) images were used over the LWREW and CRPRW study areas, respectively.

3. Methods

3.1. Satellite image processing

The AIRSAR data were initially in the Stokes matrix format and so the synthesized and decompressed procedures were applied to derive σ^0. By doing so, the radar data were available in C-band and HH (Horizontal Horizontal) polarization Jackson et al. (2009). A resampling process was then carried out to convert the 9.26 m spatial resolution to a 6.70 m. Finally, Digital Ortho-photo Quadrangles (DOQs) with a 1 m pixel size were used for geo-referencing. To this end, 40 points distributed throughout the scene were employed, by which a Root Mean Square Errors (RMSE) of half a pixel size (3.3 m) was obtained. The RADARSAT-1 datasets included here were mainly pre-processed by Shepherd (1997) and Wickel, Jackson, and Wood (2001). A Landsat Thematic Mapper (TM) image, acquired on 25 July 1997, was applied to geo-register the RADARSAT-1 scenes using several ground control points. Then, the RADARSAT-1 raw values were converted to σ^0 according to the methodology described in Srivastava (1999). Finally, an average σ^0 value was assigned to each sample with an area of 20 m × 30 m (Sahebi, Bonn, and Bénié 2004).

3.2. Empirical backscattering models

One of the basic empirical models used to characterize the relationship between σ^0 and soil surface parameters was presented by Attema and Ulaby (1978) as follows:

$$\sigma^0 = A + Bm_v \tag{1}$$

in which σ^0 (dB) and A (dB) are the total backscattering coefficient value and backscattering coefficient of dry soil, respectively; m_v is the volumetric SM; and B is the coefficient that indicates the sensitivity of the radar signal to SM. Subsequently, several advanced empirical models have been developed based on this basic relationship (Zribi et al. 2013). In the following sections, three of these models, as well as two new models developed in this study, are discussed in more detail.

3.2.1. The Champion model

The Champion model (Equation (2)) is a nonlinear model, developed by Champion (1996), to include θ in the basic backscattering model (see Equation (1)).

$$\sigma^0 = C_1 + C_2(\cos\theta)^{C_3} + Dm_v \tag{2}$$

where C_1, C_2, C_3 (dB) refer to the dependence of σ^0 on θ. C_1 is σ^0 of dry soil when $\theta = 90°$; C_2 is the total dynamics of soil response over $\theta = 0°$ to $60°$; and C_3 is the shape factor of the cosine function. The main limitation of this model is that it neglects the effects of other surface parameters, such as soil surface roughness, on the backscattering values.

3.2.2. The Sahebi model

Because the Champion model does not consider roughness parameters, Sahebi, Bonn, and Bénié (2004) included the effects of soil surface roughness on σ^0 by adding rms in their empirical model (Equation (3)).

$$\sigma^0 = A_1 + A_2(\cos\theta)^{A_3} + A_4 \ln(\text{rms}) + Dm_v \tag{3}$$

where A_1, A_2, A_3, A_4, and D are coefficients determined using training datasets. In Sahebi, Bonn, and Gwyn (2003), the constants of A_1, A_2, A_3, A_4, and D were calculated for a configuration of C-band and HH polarization using the nonlinear least squares method.

3.2.3. The Zribi and Dechambre model

One of the limitations of empirical models such as the Sahebi model is that they do not consider l, although several studies have demonstrated the effects of this parameter on σ^0 (Baghdadi, Holah, and Zribi 2006; Verhoest et al. 2008; Choker et al. 2017). The l parameter describes the horizontal distance over which the surface profile is autocorrelated. The effect of l on surface analysis have been investigated in several studies. For example, Davidson et al. (2003), Verhoest et al. (2008), and Zribi, Gorrab, and Baghdadi (2014) proposed l and rms as a single term or a function of surface roughness. Moreover, Baghdadi, Holah, and Zribi (2006), Choker et al. (2017), and Mirsoleimani et al. (2019) fitted an optimum parameter in which l was a function of θ, rms, and polarization type. Finally, Álvarez-Mozos, Gonzalez-Audícana, and Casalí (2007) and MirMazloumi and Sahebi (2016) considered l separately from rms.

Zribi and Dechambre (2003) developed an empirical model (the Zribi/Dechambre model, Equation (4)) to consider SM, rms height, and *l*. The authors proposed the use of $Z_{rms}(cm) = (rms^2)/l$ in their empirical model because it was challenging to separately estimate the effects of the rms height and *l* using empirical backscattering models over rough surfaces.

$$\sigma^0 = A + B \ln(Z_{rms}) + Dm_v \qquad (4)$$

3.2.4. The modified Zribi and Dechambre model

The Zribi/Dechambre model used only backscatters with $\theta = 25°$, $39°$ and, thus, their model did not result in reasonable accuracies for $\theta = 20°to25°$ and $\theta = 45°to70°$ (Zribi and Dechambre 2003). In the current study, this model was modified by (1) considering SAR data acquired with $\theta = 20°to64°$ and (2) adding minus power to Z_{rms} in the original equation (named the modified Zribi/Dechambre model) as provided in Equation (5). In this study, this was added because it was observed that $\exp(-Z_{rms})$ had highest correlation with σ^0 when compared to $\ln(Z_{rms})$.

$$\sigma^0 = A + B \exp(-Z_{rms}) + Dm_v \qquad (5)$$

3.2.5. New proposed empirical backscattering model

In this study, a new empirical backscattering model (Equation (6)) was developed to (1) consider all parameters that can affect σ^0 (i.e., SM, θ, rms and *l*) (MirMazloumi and Sahebi 2016), and (2) consider each of these parameters as a separate term within a single model. Moreover, the proposed model was assumed to be comprehensive because it was developed based on datasets collected from areas with various land cover characteristics. Compared to other empirical models, another new aspect of the proposed model is that it utilizes rms in the power of the exponential. This was because it was observed that using rms in the power of exponential increased the correlation with σ^0 compared to other forms of statistical models, such as logarithmic or linear.

$$\sigma^0 = A_1 + (\cos\theta)^{A_2} + \exp(A_3(rms)) + A_4 m_v + A_5 \ln(l) \qquad (6)$$

In which the series of *A* coefficients were calculated for band C and HH polarization using the least square method. Each term of the equation was obtained by the method proposed by Attema and Ulaby (1978), in which achieving the best function for each parameter was attempted. The correlation assessment was performed among all four parameters used in the proposed model (i.e., m_v, θ, rms and *l*) and σ^0 using different forms of regression equations, including linear, polynomial (second-order), geometrical, and logarithmic. Subsequently, the model that produced the highest correlation coefficient was selected for each term. For example, both sinusoidal and cosine functions were tested for $\theta = 20°to64°$. The data were correlated to σ^0 in the two datasets using the $\sin\theta$ function. However, σ^0 was increased by increasing θ using sinusoidal function, which was not in agreement with the fact that σ^0 from a rough surface decreases with increasing θ (Champion 1996; Sahebi, Bonn, and Gwyn 2003; Verhoest et al. 2008; Bousbih et al. 2017).

Furthermore, the cosine function provided more accurate results along with other terms in the model. Thus, more experiments over various datasets needs to be performed to confirm the use of sinusoidal function in empirical models. Therefore, cosine function was used in the proposed model (i.e., $(\cos\theta)^{A_2}$: second term in Equation (6)). Moreover, it has been extensively discussed that linear functions are the best models to relate SM to σ^0 (Champion 1996; Sahebi, Bonn, and Bénié 2004; Zribi and Dechambre 2003; Zribi, Gorrab, and Baghdadi 2014; Petropoulos, Ireland, and Barrett 2015) and, thus, a linear model was used in the fourth term of the proposed model ($A_4 m_v$). The relationship between surface roughness parameters (i.e., both rms and l) and σ^0 was the critical point due to wide range of θ and roughness, which were used in this study. The low values of θ (e.g., near to 10°) decreases the influence of soil roughness. The decreasing rate of σ^0 can be also observed after 30°(Oh, Sarabandi, and Ulaby 2004). Although surface roughness is a confounding factor on bare soil analysis, it has been reported that the backscattering from a rough surface increases with roughness (Toure et al. 1991; Oh, Sarabandi, and Ulaby 2004; Verhoest et al. 2008). Thus, finding a straightforward correlation between (rms)/l and σ^0 for the datasets were complicated. To find the most appropriate mathematical function for soil surface parameters, sinusoidal and cosine functions were initially tested, although this did not result in a high correlation with. However, logarithmic functions resulted in a high correlation coefficient. For instance, an exponential function resulted the best fitting for rms (see $\exp(A_3(\text{rms}))$ in Equation (6)). It is also worth noting that the coefficient (A_3) was used in the power of the exponential function to increase the correlation and, thus, to improve the prediction accuracy of the model.

3.3. Model development and accuracy assessment

All the *in-situ* data (see subsection *In-situ datasets*) were randomly divided into training (75%) and test (25%) datasets. The training data were used to develop the empirical models and, in fact, to calculate the coefficients of each model using least square method. In total, 39 and 29 samples of LWREW and CRPRW were, respectively, selected to train the models. The test data (13 and 10 samples of LWREW and CRPRW, respectively) were also employed for accuracy assessment through calculating the Mean Absolute Error (MAE), Root Mean Square Error (RMSE), and unbiased RMSE (ubRMSE) metrics (or the error standard deviation).

$$\text{MAE} = \frac{1}{N}\sum_{i=1}^{N}\left|\sigma_{\text{est}}^0(i) - \sigma_{\text{im}}^0(i)\right| \tag{7}$$

$$\text{ubRMSE} = \sqrt{\frac{1}{N}\left(\sum_{i=1}^{N}\left(\sigma_{\text{est}}^0(i) - \overline{\sigma_{\text{est}}^0}\right) - \sum_{i=1}^{N}\left(\sigma_{\text{im}}^0(i) - \overline{\sigma_{\text{im}}^0}\right)\right)^2} \tag{8}$$

$$\text{RMSE} = \sqrt{\frac{1}{N}\sum_{i=1}^{N}\left(\sigma_{\text{est}}^0(i) - \sigma_{\text{im}}^0(i)\right)^2} \tag{9}$$

$$RMSE^2 = (ubRMSE)^2 + b^2 \tag{10}$$

$$b = \frac{1}{N}\sum_{i=1}^{N}\left(\sigma_{est}^0(i) - \sigma_{im}^0(i)\right) \tag{11}$$

where N is the number of points with both estimated backscattering coefficient from models (σ_{est}^0) and that of extracted from and image (σ_{im}^0). The overbar represents the average of the variables. The ubRMSE measures the RMSE excluding the bias (b). It is worth noting that RMSE is critically undermined if there are biases in either the average or the amplitude of fluctuations in the estimation (Taylor 2001; Entekhabi et al. 2010; Liu, Yang, and Yue 2018). Thus, the mean-bias can easily be removed by defining the unbiased RMSE, which implies RMSE $\geq |b|$ and emphasizes on the deficiency of the RMSE in the presence of mean-bias.

The development of models and accuracy assessment included the following:

(1) The accuracies of the Champion, Sahebi, and Zribi/Dechambre models with the corresponding original coefficients were assessed using the test data.
(2) The coefficients of the Champion, Sahebi, and Zribi/Dechambre models were re-calculated using the training data and least square method and the accuracies of these refined models were then evaluated using the test data.
(3) The coefficients of the modified Zribi/Dechambre model (Equation (5)) were calculated using the training data and least square method and, then, its accuracy was assessed using the test data.
(4) The new proposed model (Equation (6)) was developed by calculating its coefficients using the training datasets. Then, its accuracy was evaluated using the test data.

4. Results and discussion

The procedure described in subsection *Empirical backscattering models* was applied to develop each empirical model, discussed by followed, and to obtain the level of accuracy. Consequently, all empirical backscattering models, including their coefficients and accuracy parameters, are provided in Tables 3–7. Additionally, the distribution of the estimated σ^0 from each model versus the σ^0 obtained from the AIRSAR and RADARSAT-1 datasets for the test data are illustrated in Figure 2.

As clear from Figure 2(a,b), the σ^0 values obtained from the calibrated Champion model are closer to the 1:1 line compared to those obtained from the original model. In fact, the original Champion model significantly underestimated and overestimated σ^0 values over LWREW and CRPRW, respectively. This can be also observed in Table 3, in which the MAE, RMSE and ubRMSE errors for the calibrated Champion model is considerably lower than those of the original model. Additionally, considerable differences were observed for the values of C_2 and D in the original and calibrated Champion model (see Table 3). This may be due to the local characteristics of each study area (Champion 1996). As explained in Champion (1996), the difference could be due to the influence of $k \times$ (rms) and $k \times l$ on C_2 (k is the wavenumber), which expresses roughness values, and their values are about 0.7 and 3.0 in the original Champion model. It was reported that there is

Table 3. The accuracy of the Champion model obtained from the original coefficients of the model and the calibrated coefficients using the *in-situ* data (training data) in this study.

Study area	Datasets	Coefficient	C_1	C_2	C_3	D	MAE (dB)	RMSE (dB)	ubRMSE (dB)
LWREW	AIRSAR	Original	−29.20	27.20	2.80	17.42	6.89	2.93	6.64
		Calibrated	−16.25	0.03	1.58	−0.54	1.81	1.40	1.14
CRPRW	RADARSAT-1	Original	−29.20	27.20	2.80	17.42	6.09	2.60	5.50
		Calibrated	−19.45	78.27	−2.48	43.05	1.80	1.64	2.44

Table 4. The accuracy of the Sahebi model obtained from the original coefficients of the model and the calibrated coefficients using the *in-situ* data (training data) in this study.

Study area	Datasets	Coefficient	A_1	A_2	A_3	A_4	D	MAE (dB)	RMSE (dB)	ubRMSE (dB)
LWREW	AIRSAR	Original	−27.14	17.50	0.25	−0.31	1.85	3.48	2.48	2.97
		Calibrated	−8.38	42.50	52.09	−2.41	−0.15	2.95	1.80	1.60
CRPRW	RADARSAT-1	Original	−27.14	17.50	0.25	−0.31	1.85	3.02	1.83	2.41
		Calibrated	−14.22	26.72	1.00	−1.41	−0.70	2.38	1.62	1.74

Table 5. The accuracy of the Zribi/Dechambre model obtained from the original coefficients of the model and the calibrated coefficients using the *in-situ* data (training data) in this study.

Study area	Datasets	Coefficient	A	B	D	MAE (dB)	RMSE (dB)	ubRMSE (dB)
LWREW	AIRSAR	Original	−13.30	1.56	0.22	1.98	1.46	1.34
		Calibrated	−14.70	0.21	2.36	1.42	1.24	0.69
CRPRW	RADARSAT-1	Original	−13.30	1.56	0.22	5.37	2.44	4.78
		Calibrated	−16.20	2.99	38.96	2.44	1.64	1.80

Table 6. The accuracy of the modified Zribi/Dechambre model proposed in this study.

Study area	Datasets	A	B	D	MAE (dB)	RMSE (dB)	ubRMSE (dB)
LWREW	AIRSAR	−12.50	−3.82	2.63	1.33	1.20	0.58
CRPRW	RADARSAT-1	−16.72	−4.22	42.93	2.30	1.59	1.65

Table 7. The accuracy of the new proposed empirical backscattering model with and without correlation length (A_5).

Study area	Datasets	A_1	A_2	A_3	A_4	A_5	MAE (dB)	RMSE (dB)	ubRMSE (dB)
LWREW	AIRSAR	−11.94	26.23	0.26	2.08	−2.38	1.36	1.20	1.16
		−14.96	42.57	0.61	0.17	0.00	3.03	1.82	1.80
CRPRW	RADARSAT-1	−5.21	51.40	0.38	0.15	−2.83	3.04	1.83	1.69
		−14.59	40.09	0.60	0.12	0.00	3.50	1.97	1.54

a negative relationship between $k \times (\text{rms})$ and C_2, wherein as the latter decreases as the former increases (Champion 1996).

Figure 2(c,d) illustrates the σ^0 derived from the original and calibrated Sahebi model (see Table 4 for the coefficient and the accuracies for the model with original and calibrated coefficients). As is clear, the accuracy of the calibrated model was higher than that of the original model. For instance, the RMSE values were 1.80 dB and 2.48 dB in the LWREW study area for the calibrated and original Sahebi models, respectively. The most important reason is that the calibrated model was developed based on the datasets collected in this study. Another reason might be due to the large difference between θ in these two cases. The original coefficients were calculated using the data from the Chateauguay site acquired with 20° to 47° angles; however, θ was between 47° and 64°
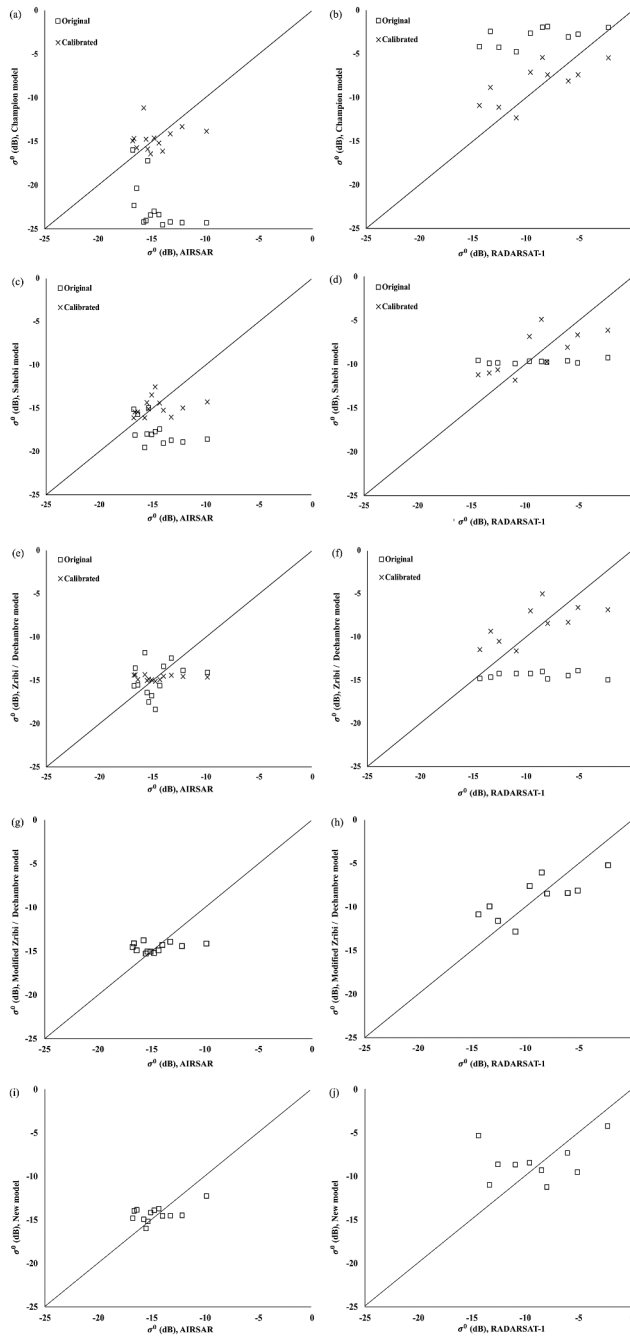
Figure 2. Comparison of the backscattering coefficients (σ^0) obtained from the SAR datasets and different empirical backscattering models. AIRSAR and RADARSAT-1 images were acquired from 13 samples of the Little Washita Experimental Watershed (LWREW) and 10 samples of Chateauguay River and Pike River watersheds (CRPRW) study areas, respectively. The diagonals are 1:1.

in this study. Overall, the accuracy increased in both datasets using the calibrated model (Table 4); however, better improvement was observed in the CRPRW study region, in which θ was smaller than that of the LWREW study area. Therefore, it was concluded that the Sahebi model more accurately estimates σ^0 when $\theta < 47°$. Finally, the Sahebi model did not underestimate to the same degree as the Champion model when σ^0 was between −15 dB and −10 dB.

Figure 2(e–h) and Tables 5–6 provide the results of both the original and calibrated Zribi/Dechambre models, as well as the modified Zribi/Dechambre model proposed in this study. Comparing the accuracy parameters provided in Tables 5 and 6, it was observed that the modified Zribi/Dechambre model had the highest accuracy in estimating σ^0, followed by the calibrated and original Zribi/Dechambre models, respectively. Over LWREW, a slight overestimation of approximately 0.5 dB was observed when σ^0 was between −18 dB and −15, while a slight underestimation was observed for greater σ^0 values except when $\sigma^0 = -10$ dB. Furthermore, Figure 2(e–h) shows the sensitivity of the original Zribi/Dechambre model to small θ values, as the original model underestimated all σ^0 values in RADARSAT-1 data acquired over CRPRW. It was also observed that the distribution of the estimated σ^0 values obtained from the modified Zribi/Dechambre model was more accurate than those of the original and calibrated Zribi/Dechambre models.

Figure 2(i,j) and Table 7 provide the results of the backscattering model proposed in this study. As clearly illustrated in Figure 2, the estimated σ^0 values from the proposed model were closer to the centreline compared to Champion, Sahebi, and Zribi/Dechambre models, indicating the higher accuracy of the proposed model. This was also observed by comparing all the results provided in Table 3 to 5 and 7, where the proposed model had the lowest MAE, RMSE and ubRMSE values. For instance, the RMSE errors decreased by between 0.10 dB and 1.50 dB for the LWREW and between 0.15 dB to 1.00 dB for the CRPRW study areas compared to the Champion, Sahebi, and Zribi/Dechambre empirical models. As another example, the high overestimation and underestimation of σ^0 values when using the Champion and Sahebi models were improved by the new proposed model (compare Figure 2(a–d,i,j)). However, the new backscattering model slightly overestimated and underestimated σ^0 by up to 1 dB in some cases.

The modified Zribi/Dechambre model provided the smallest metrics in Table 3 to 7, where estimated values were the closest results to the centreline in Figure 2. The MAE, RMSE, and ubRMSE of this model were, respectively, 1.33, 1.20, and 0.58 over the LWREW study area; and they were, respectively, 2.30, 1.59, and 1.65 over the CRPRW study area. According to the results in Tables 3–6, significant differences were observed for four models (the Champion, Sahebi, modified and original Zribi/Dechambre) in the two datasets. For instance, there were 40 and 36 values differences in D in the modified and Zribi/Dechambre models, respectively. Additionally, considerable differences were obtained in the Champion and Sahebi models. However, in the new proposed model, the model coefficients values, which were calibrated using field data, remained stable in the two datasets. The average variations of datasets coefficients were approximately 7, which was lower two, three, three, and five times compared to other models. Therefore,
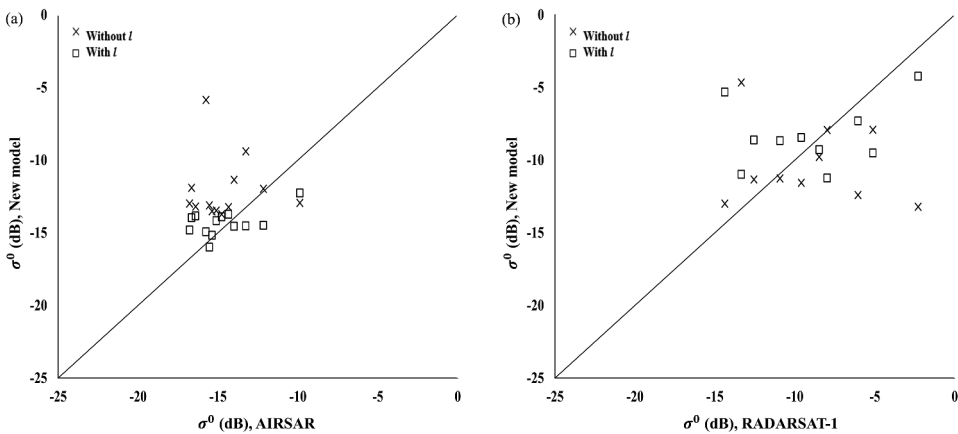
Figure 3. Comparison between the backscattering coefficients (σ^0) obtained from the SAR datasets and the new proposed empirical backscattering model when correlation length (l) was considered and removed. AIRSAR and RADARSAT-1 images were acquired from 13 samples of the Little Washita Experimental Watershed (LWREW) and 10 samples of Chateauguay River and Pike River watersheds (CRPRW) study areas, respectively. The diagonals are 1:1.

differences reflected the necessity of the calibration of the four models, which is not always practical.

Another experiment carried out in this study was investigating the importance of l in improving the accuracy of estimating σ^0, and the results are demonstrated in Table 7 and Figure 3. Specifically, l was removed from the proposed model and the accuracy of the model was recalculated and then compared with that of the original proposed model. According to Table 7, the accuracy of the proposed model decreased when l was removed. For instance, RMSE increased from 1.20 dB to 1.82 dB in the LWREW study area and it increased from 1.83 dB to 1.97 dB in the CRPRW study region when l was removed. Most studies discussed in *the Zribi and Dechambre model* section, exploited surface responses using exponential correlation function, while the inverse function of exponential (logarithm) performed efficiently over the datasets of this study. This showed the importance of considering l as an independent parameter to highlight its effect. It could be concluded that since removing l decreased the estimation capability, the effects of l might be relatively limited by describing l as a function of other independent parameters, which have their own limitations. Therefore, l could affect the backscattering models by choosing a proper function and there are four important parameters that can affect σ^0 values in a SAR images (i.e., SM, θ, rms and l), all of which should be considered in backscattering models to achieve the highest possible accuracies.

5. Conclusion

SAR systems acquire valuable datasets from which soil surface parameters may be derived using backscattering models. The objectives of this study were to (1) calibrate several empirical backscattering models, including the Champion, Sahebi and Zribi/Dechambre models, and (2) propose two new models, including the modified Zribi/Dechambre and

a novel model proposed in this study, to accurately estimate σ^0 values. Two SAR datasets, acquired by AIRSAR and RADARSAT-1, over two study areas with different soil characteristics were used to evaluate the accuracy of each model. Both the original and calibrated Champion, Sahebi and Zribi/Dechambre models were investigated in this study, and it was concluded that the calibrated models more accurately estimated σ^0 over the study areas. Moreover, it was concluded that the modified Zribi/Dechambre model developed in this study had the highest accuracy in estimating σ^0 values compared to all models evaluated in this study. However, the new proposed empirical model had higher stability in estimating the coefficients over two datasets, i.e. the least differences of the estimated coefficients for two datasets indicated that the new proposed model remained stable in the two datasets. Thus, the new proposed model can be potentially utilized over other datasets. Finally, it was concluded that all important soil surface parameters and SAR configuration parameters that can affect σ^0, including l, should be considered in any empirical model developed to obtain the highest possible accuracy. This is why multiple previous studies have implemented the correlation length using exponential function relating to other parameters (e.g., rms, θ, polarization) based on IEM model modifications (Baghdadi et al. 2004; Baghdadi, Holah, and Zribi 2006; Baghdadi et al. 2012; Choker et al. 2017; El Hajj et al. 2019; Mirsoleimani et al. 2019). Although the effect of vertical soil roughness has been examined exponentially, a logarithmic function was proposed in this study to exploit the horizontal impact. It was tried to produce an accurate empirical model by (1) calibrating the coefficients of the original models through fitting/investigating different forms of statistical models (e.g., exponential, linear, and logarithmic), and (2) considering the well-known relationships between soil surface parameters and σ^0 (e.g. backscattering from a rough surface increases with roughness and backscattering from a rough surface decreases with increasing θ). However, considering both facts together was challenging and resulted in a limitation in improving the accuracy of the proposed model. Moreover, finding the most optimal coefficients for the proposed model was challenging considering the wide range of parameters of the datasets, which were used in this study. Finally, the unknown effects related to the nature of the study area and radar noise range might disturb empirical estimations in this study. Since all the experiments in this study were performed using SAR data with C-band and HH polarizations, it is suggested that future studies calibrate previous empirical models and evaluate the accuracy of the proposed models for SAR data with other bands and polarizations types (i.e., L-, P-, and X-band/VV (Vertical Vertical) and VH (Vertical Horizontal) polarizations).

Acknowledgements

Disclosure statement

No potential conflict of interest was reported by the authors.

ORCID

S. Mohammad Mirmazloumi http://orcid.org/0000-0001-5310-5859
Mahmod Reza Sahebi http://orcid.org/0000-0001-7742-3974
Meisam Amani http://orcid.org/0000-0002-9495-4010

References

Álvarez-Mozos, J., M. Gonzalez-Audícana, and J. Casalí. 2007. "Evaluation of Empirical and Semi-empirical Backscattering Models for Surface Soil Moisture Estimation." *Canadian Journal of Remote Sensing* 33 (3): 176–188. doi:10.5589/m07-024.

Amani, M., B. Salehi, S. Mahdavi, B. Brisco, and M. Shehata. 2018. "A Multiple Classifier System to Improve Mapping Complex Land Covers: A Case Study of Wetland Classification Using SAR Data in Newfoundland, Canada." *International Journal of Remote Sensing* 39 (21): 7370–7383. doi:10.1080/01431161.2018.1468117.

Amani, M., B. Salehi, S. Mahdavi, J. Granger, and B. Brisco. 2017. "Wetland Classification in Newfoundland and Labrador Using Multi-source SAR and Optical Data Integration." *GIScience & Remote Sensing* 54 (6): 779–796. doi:10.1080/15481603.2017.1331510.

Attema, E. P. W., and F. T. Ulaby. 1978. "Vegetation Modeled as a Water Cloud." *Radio Science* 13 (2): 357–364. doi:10.1029/RS013i002p00357.

Azimi, S., A. B. Dariane, S. Modanesi, B. Bauer-Marschallinger, R. Bindlish, W. Wagner, and C. Massari. 2020. "Assimilation of Sentinel 1 and SMAP–based Satellite Soil Moisture Retrievals into SWAT Hydrological Model: The Impact of Satellite Revisit Time and Product Spatial Resolution on Flood Simulations in Small Basins." *Journal of Hydrology* 581: 124367.

Baghdadi, N., M. Aubert, and M. Zribi. 2011. "Use of TerraSAR-X Data to Retrieve Soil Moisture over Bare Soil Agricultural Fields." *IEEE Geoscience and Remote Sensing Letters* 9 (3): 512–516. doi:10.1109/LGRS.2011.2173155.

Baghdadi, N., M. Aubert, O. Cerdan, L. Franchistéguy, C. Viel, M. Eric, M. Zribi, and J. F. Desprats. 2007. "Operational Mapping of Soil Moisture Using Synthetic Aperture Radar Data: Application to the Touch Basin (France)." *Sensors* 7 (10): 2458–2483. doi:10.3390/s7102458.

Baghdadi, N., N. Holah, and M. Zribi. 2006. "Calibration of the Integral Equation Model for SAR Data in C-band and HH and VV Polarizations." *International Journal of Remote Sensing* 27 (4): 805–816. doi:10.1080/01431160500212278.

Baghdadi, N., R. Cresson, E. Pottier, M. Aubert, M. Mehrez, A. Jacome, and S. Benabdallah. 2012. "A Potential Use for the C-band Polarimetric SAR Parameters to Characterize the Soil Surface over Bare Agriculture Fields." *IEEE Transactions on Geoscience and Remote Sensing* 50 (10): 3844–3858. doi:10.1109/TGRS.2012.2185934.

Baghdadi, N. I., M. Z. Gherboudj, M. Sahebi, C. King, and F. Bonn. 2004. "Semi-empirical Calibration of the IEM Backscattering Model Using Radar Images and Moisture and Roughness Field Measurements." *International Journal of Remote Sensing* 25 (18): 3593–3623. doi:10.1080/01431160310001654392.

Barrett, B. W., E. Dwyer, and P. Whelan. 2009. "Soil Moisture Retrieval from Active Spaceborne Microwave Observations: An Evaluation of Current Techniques." *Remote Sensing* 1 (3): 210–242. doi:10.3390/rs1030210.

Baup, F., E. Mougin, P. De Rosnay, P. Hiernaux, F. Frappart, P.-L. Frison, M. Zribi, and J. Viarre. 2011. "Mapping Surface Soil Moisture over the Gourma Mesoscale Site (Mali) by Using ENVISAT ASAR Data."

Beaulieu, N., G. Leclerc, and Y. Moisan. 1995. "Détermination de la rugosité de surface par des méthodes accessibles." *Canadian Journal of Remote Sensing* 21 (2): 198–203. doi:10.1080/07038992.1995.10874613.

Berardino, P., G. Fornaro, R. Lanari, and E. Sansosti. 2002. "A New Algorithm for Surface Deformation Monitoring Based on Small Baseline Differential SAR Interferograms." *IEEE Transactions on Geoscience and Remote Sensing* 40 (11): 2375–2383. doi:10.1109/TGRS.2002.803792.

Bousbih, S., M. Zribi, Z. Lili-Chabaane, N. Baghdadi, M. El Hajj, Q. Gao, and B. Mougenot. 2017. "Potential of Sentinel-1 Radar Data for the Assessment of Soil and Cereal Cover Parameters." *Sensors* 17 (11): 2617. doi:10.3390/s17112617.

Callens, M., N. E. C. Verhoest, and M. W. J. Davidson. 2006. "Parameterization of Tillage-induced Single-scale Soil Roughness from 4-m Profiles." *IEEE Transactions on Geoscience and Remote Sensing* 44 (4): 878–888. doi:10.1109/TGRS.2005.860488.

Chai, X., T. Zhang, Y. Shao, H. Gong, L. Liu, and K. Xie. 2015. "Modeling and Mapping Soil Moisture of Plateau Pasture Using RADARSAT-2 Imagery." *Remote Sensing* 7 (2): 1279–1299. doi:10.3390/rs70201279.

Champion, I. 1996. "Simple Modelling of Radar Backscattering Coefficient over a Bare Soil: Variation with Incidence Angle, Frequency and Polarization." *International Journal of Remote Sensing* 17 (4): 783–800.

Choker, M., N. Baghdadi, M. Zribi, M. El Hajj, S. Paloscia, N. E. Verhoest, H. Lievens, and F. Mattia. 2017. "Evaluation of the Oh, Dubois and IEM Backscatter Models Using a Large Dataset of SAR Data and Experimental Soil Measurements." *Water* 9 (1): 38. doi:10.3390/w9010038.

Davidson, M. W. J., F. Mattia, G. Satalino, N. E. C. Verhoest, T. Le Toan, M. Borgeaud, J. M. B. Louis, and E. Attema. 2003. "Joint Statistical Properties of RMS Height and Correlation Length Derived from Multisite 1-m Roughness Measurements." *IEEE Transactions on Geoscience and Remote Sensing* 41 (7): 1651–1658. doi:10.1109/TGRS.2003.813361.

Dubois, P. C., J. Van Zyl, and T. Engman. 1995. "Measuring Soil Moisture with Imaging Radars." *IEEE Transactions on Geoscience and Remote Sensing* 33 (4): 915–926. doi:10.1109/36.406677.

El Hajj, M., N. Baghdadi, J. P. Wigneron, M. Zribi, C. Albergel, J. C. Calvet, and I. Fayad. 2019. "First Vegetation Optical Depth Mapping from Sentinel-1 C-band SAR Data over Crop Fields." *Remote Sensing* 11 (23): 2769. doi:10.3390/rs11232769.

Entekhabi, D., R. H. Reichle, R. D. Koster, and W. T. Crow. 2010. "Performance Metrics for Soil Moisture Retrievals and Application Requirements." *Journal of Hydrometeorology* 11 (3): 832–840. doi:10.1175/2010JHM1223.1.

Ezzahar, J., N. Ouaadi, M. Zribi, J. Elfarkh, G. Aouade, S. Khabba, S. Er-Raki, A. Chehbouni, and L. Jarlan. 2020. "Evaluation of Backscattering Models and Support Vector Machine for the Retrieval of Bare Soil Moisture from Sentinel-1 Data." *Remote Sensing* 12 (1): 72. doi:10.3390/rs12010072.

Fung, A. K., Z. Li, and K.-S. Chen. 1992. "Backscattering from a Randomly Rough Dielectric Surface." *IEEE Transactions on Geoscience and Remote Sensing* 30 (2): 356–369. doi:10.1109/36.134085.

Gherboudj, I., R. Magagi, A. A. Berg, and B. Toth. 2011. "Soil Moisture Retrieval over Agricultural Fields from Multi-polarized and Multi-angular RADARSAT-2 SAR Data." *Remote Sensing of Environment* 115 (1): 33–43. doi:10.1016/j.rse.2010.07.011.

Hachani, A., M. Ouessar, S. Paloscia, E. Santi, and S. Pettinato. 2019. "Soil Moisture Retrieval from Sentinel-1 Acquisitions in an Arid Environment in Tunisia: Application of Artificial Neural Networks Techniques." *International Journal of Remote Sensing* 40 (24): 9159–9180. doi:10.1080/01431161.2019.1629503.

Hajnsek, I., E. Pottier, and S. R. Cloude. 2003. "Inversion of Surface Parameters from Polarimetric SAR." *IEEE Transactions on Geoscience and Remote Sensing* 41 (4): 727–744. doi:10.1109/TGRS.2003.810702.

Hajnsek, I., K. P. Papathanassiou, and S. R. Cloude. 2001. "L-and P-band for Surface Parameter Estimation." In *IGARSS 2001. Scanning the Present and Resolving the Future. Proceedings. IEEE 2001 International Geoscience and Remote Sensing Symposium (Cat. No. 01CH37217)*, vol. 6, 2775–2777. Sydney, NSW, Australia: IEEE.

Holah, N., N. Baghdadi, M. Zribi, A. Bruand, and C. King. 2005. "Potential of ASAR/ENVISAT for the Characterization of Soil Surface Parameters over Bare Agricultural Fields." *Remote Sensing of Environment* 96 (1): 78–86. doi:10.1016/j.rse.2005.01.008.

Hosseini, M., and M. R. Saradjian. 2011. "Soil Moisture Estimation Based on Integration of Optical and SAR Images." *Canadian Journal of Remote Sensing* 37 (1): 112–121. doi:10.5589/m11-015.

Iodice, A., A. Natale, and D. Riccio. 2011. "Retrieval of Soil Surface Parameters via a Polarimetric Two-scale Model." *IEEE Transactions on Geoscience and Remote Sensing* 49 (7): 2531–2547.

Jackson, T. J., A. J. Gasiewski, A. Oldak, E. G. Marian Klein, A. Y. Njoku, S. Christiani, and R. Bindlish. 2002. "Soil Moisture Retrieval Using the C-band Polarimetric Scanning Radiometer during the Southern Great Plains 1999 Experiment." *IEEE Transactions on Geoscience and Remote Sensing* 40 (10): 2151–2161. doi:10.1109/TGRS.2002.802480.

Jackson, T. J., and M. H. Cosh. 2006. "SMEX03 Regional Ground Soil Moisture Data: Oklahoma."

Jackson, T. J., R. Bindlish, and R. Van der Velde. 2009. *SMEX03 Airborne Synthetic Aperture Radar (AIRSAR) Data: Oklahoma, Version 1*. Boulder, Colorado: NASA National Snow and Ice Data Center Distributed Active Archive Center.

Kirimi, F., D. N. Kuria, F. Thonfeld, E. Amler, K. Mubea, S. Misana, and G. Menz. 2016. "Influence of Vegetation Cover on the Oh Soil Moisture Retrieval Model: A Case Study of the Malinda Wetland, Tanzania."

Li, X., Y. Zhou, P. Gong, K. C. Seto, and N. Clinton. 2020. "Developing a Method to Estimate Building Height from Sentinel-1 Data." *Remote Sensing of Environment* 240: 111705. doi:10.1016/j.rse.2020.111705.

Liu, Y., Y. Yang, and X. Yue. 2018. "Evaluation of Satellite-based Soil Moisture Products over Four Different Continental In-situ Measurements." *Remote Sensing* 10 (7): 1161. doi:10.3390/rs10071161.

Mahdavi, S., B. Salehi, M. Amani, J. E. Granger, B. Brisco, W. Huang, and A. Hanson. 2017. "Object-based Classification of Wetlands in Newfoundland and Labrador Using Multi-temporal PolSAR Data." *Canadian Journal of Remote Sensing* 43 (5): 432–450. doi:10.1080/07038992.2017.1342206.

McNairn, H., J. B. Boisvert, D. J. Major, Q. H. J. Gwyn, R. J. Brown, and A. M. Smith. 1996. "Identification of Agricultural Tillage Practices from C-band Radar Backscatter." *Canadian Journal of Remote Sensing* 22 (2): 154–162. doi:10.1080/07038992.1996.10874649.

MirMazloumi, S. M., and M. R. Sahebi. 2016. "Assessment of Different Backscattering Models for Bare Soil Surface Parameters Estimation from SAR Data in Band C, L and P." *European Journal of Remote Sensing* 49 (1): 261–278. doi:10.5721/EuJRS20164915.

Mirsoleimani, H. R., M. R. Sahebi, N. Baghdadi, and M. E. Hajj. 2019. "Bare Soil Surface Moisture Retrieval from Sentinel-1 SAR Data Based on the Calibrated IEM and Dubois Models Using Neural Networks." *Sensors* 19 (14): 3209. doi:10.3390/s19143209.

Notarnicola, C., and R. Solorza. 2014. "Integration of Remotely Sensed Images and Electromagnetic Models into a Bayesian Approach for Soil Moisture Content Retrieval: Methodology and Effect of Prior Information." *Sensors* 1 (4): 5–6

Oh, Y. 2004. "Quantitative Retrieval of Soil Moisture Content and Surface Roughness from Multipolarized Radar Observations of Bare Soil Surfaces." *IEEE Transactions on Geoscience and Remote Sensing* 42 (3): 596–601. doi:10.1109/TGRS.2003.821065.

Oh, Y., K. Sarabandi, and F. T. Ulaby. 1992. "An Empirical Model and an Inversion Technique for Radar Scattering from Bare Soil Surfaces." *IEEE Transactions on Geoscience and Remote Sensing* 30 (2): 370–381. doi:10.1109/36.134086.

Paloscia, S., P. Pampaloni, S. Pettinato, and E. Santi. 2008. "A Comparison of Algorithms for Retrieving Soil Moisture from ENVISAT/ASAR Images." *IEEE Transactions on Geoscience and Remote Sensing* 46 (10): 3274–3284. doi:10.1109/TGRS.2008.920370.

Petropoulos, G. P., G. Ireland, and B. Barrett. 2015. "Surface Soil Moisture Retrievals from Remote Sensing: Current Status, Products & Future Trends." *Physics and Chemistry of the Earth, Parts A/B/C* 83: 36–56. doi:10.1016/j.pce.2015.02.009.

Rao, S. S., S. N. Das, M. S. S. Nagaraju, M. V. Venugopal, P. Rajankar, P. Laghate, M. S. Reddy, A. K. Joshi, and J. R. Sharma. 2013. "Modified Dubois Model for Estimating Soil Moisture with Dual Polarized SAR Data." *Journal of the Indian Society of Remote Sensing* 41 (4): 865–872. doi:10.1007/s12524-013-0274-3.

Sahebi, M. R., F. Bonn, and G. B. Bénié. 2004. "Neural Networks for the Inversion of Soil Surface Parameters from Synthetic Aperture Radar Satellite Data." *Canadian Journal of Civil Engineering* 31 (1): 95–108. doi:10.1139/l03-079.

Sahebi, M. R., F. Bonn, and Q. H. J. Gwyn. 2003. "Estimation of the Moisture Content of Bare Soil from RADARSAT-1 SAR Using Simple Empirical Models." *International Journal of Remote Sensing* 24 (12): 2575–2582. doi:10.1080/0143116031000072948.

Shepherd, N. 1997. "Extraction of Beta Nought and Sigma Nought from RADARSAT CDPF Products, Report No." *AS97–5001* 30.

Srivastava, S. K., R. K. Hawkins, T. I. Lukowski, B. T. Banik, M. Adamovic, and W. C. Jefferies. 1999. "RADARSAT image quality and calibration—Update." *Advances in Space Research* 23 (8): 1487–1496

Sun, H., M. Shimada, and F. Xu. 2017. "Recent Advances in Synthetic Aperture Radar Remote Sensing —Systems, Data Processing, and Applications." *IEEE Geoscience and Remote Sensing Letters* 14 (11): 2013–2016. doi:10.1109/LGRS.2017.2747602.

Taylor, K. E. 2001. "Summarizing Multiple Aspects of Model Performance in a Single Diagram." *Journal of Geophysical Research: Atmospheres* 106 (D7): 7183–7192. doi:10.1029/2000JD900719.

Tofani, V., F. Raspini, F. Catani, and N. Casagli. 2013. "Persistent Scatterer Interferometry (PSI) Technique for Landslide Characterization and Monitoring." *Remote Sensing* 5 (3): 1045–1065. doi:10.3390/rs5031045.

Toure, A., K. P. B. Thomson, G. Edwards, R. J. Brown, and B. Brisco. 1991. "Applying the MIMICS Backscattering Model in an Agricultural Context." *Canadian Journal of Remote Sensing* 17 (4): 339–347. doi:10.1080/07038992.1991.10855303.

Ulaby, F. T., P. C. Dubois, and J. Van Zyl. 1996. "Radar Mapping of Surface Soil Moisture." *Journal of Hydrology* 184 (1–2): 57–84. doi:10.1016/0022-1694(95)02968-0.

Ulaby, F. T., and P. P. Batlivala. 1976. "Optimum Radar Parameters for Mapping Soil Moisture." *IEEE Transactions on Geoscience Electronics* 14 (2): 81–93. doi:10.1109/TGE.1976.294414.

Ulaby, F. T., R. K. Moore, and A. K. Fung. 1982. "Microwave Remote Sensing Active and Passive-volume II: Radar Remote Sensing and Surface Scattering and Enission Theory. No. BOOK." Addison-Wesley Publishing CompanyAdvanced Book Program/World Science Division.

Ulaby, F. T., R. K. Moore, and A. K. Fung. 1986. "Microwave Remote Sensing: Active and Passive. Volume 3-From Theory to Applications."

Verhoest, N. E. C., H. Lievens, W. Wagner, J. Álvarez-Mozos, M. S. Moran, and F. Mattia. 2008. "On the Soil Roughness Parameterization Problem in Soil Moisture Retrieval of Bare Surfaces from Synthetic Aperture Radar." *Sensors* 8 (7): 4213–4248. doi:10.3390/s8074213.

Wang, L., and J. J. Qu. 2009. "Satellite Remote Sensing Applications for Surface Soil Moisture Monitoring: A Review." *Frontiers of Earth Science in China* 3 (2): 237–247. doi:10.1007/s11707-009-0023-7.

Wickel, A. J., T. J. Jackson, and E. F. Wood. 2001. "Multitemporal Monitoring of Soil Moisture with RADARSAT SAR during the 1997 Southern Great Plains Hydrology Experiment." *International Journal of Remote Sensing* 22 (8): 1571–1583. doi:10.1080/01431160120291.

Zakharov, I., M. Kapfer, J. Hornung, S. Kohlsmith, T. Puestow, M. Howell, and M. D. Henschel. 2020. "Retrieval of Surface Soil Moisture from Sentinel-1 Time Series for Reclamation of Wetland Sites." *IEEE Journal of Selected Topics in Applied Earth Observations and Remote Sensing* 13: 3569–3578. doi:10.1109/JSTARS.2020.3004062.

Zhang, X., H. Zhang, C. Wang, Y. Tang, B. Zhang, F. Wu, J. Wang, and Z. Zhang. 2020. "Active Layer Thickness Retrieval over the Qinghai-Tibet Plateau Using Sentinel-1 Multitemporal InSAR Monitored Permafrost Subsidence and Temporal-Spatial Multilayer Soil Moisture Data." *IEEE Access* 8: 84336–84351. doi:10.1109/ACCESS.2020.2988482.

Zribi, M., A. Gorrab, and N. Baghdadi. 2014. "A New Soil Roughness Parameter for the Modelling of Radar Backscattering over Bare Soil." *Remote Sensing of Environment* 152: 62–73. doi:10.1016/j.rse.2014.05.009.

Zribi, M., A. Gorrab, N. Baghdadi, Z. Lili-Chabaane, and B. Mougenot. 2013. "Influence of Radar Frequency on the Relationship between Bare Surface Soil Moisture Vertical Profile and Radar Backscatter." *IEEE Geoscience and Remote Sensing Letters* 11 (4): 848–852. doi:10.1109/LGRS.2013.2279893.

Zribi, M., and M. Dechambre. 2003. "A New Empirical Model to Retrieve Soil Moisture and Roughness from C-band Radar Data." *Remote Sensing of Environment* 84 (1): 42–52. doi:10.1016/S0034-4257(02)00069-X.

Zribi, M. V., C. O. Taconet, J. Paillé, and P. Boissard. 2000. "Characterisation of the Soil Structure and Microwave Backscattering Based on Numerical Three-dimensional Surface Representation: Analysis with a Fractional Brownian Model." *Remote Sensing of Environment* 72 (2): 159–169. doi:10.1016/S0034-4257(99)00097-8.